Proper ferroelastic transitions in two dimensions: Anisotropic long-range kernels, domain wall orientations, and microstructure

Dorian M. Hatch,[1] Turab Lookman,[2] Avadh Saxena,[2] and Subodh R. Shenoy[3]
[1]*Department of Physics and Astronomy, Brigham Young University, Provo, Utah 84602, USA*
[2]*Theoretical Division, Los Alamos National Laboratory, Los Alamos, New Mexico 87545, USA*
[3]*Abdus Salam International Centre for Theoretical Physics, Trieste 34100, Italy*
(Received 8 August 2002; revised manuscript received 20 June 2003; published 5 September 2003)

For structural transitions with strain serving as the transition primary order parameter (proper ferroelastics), we obtain 23 proper ferroelastic transitions in two dimensions and derive distinct ''elastic compatibility'' kernels that specify anisotropic, long-range order-parameter interactions. These kernels influence possible domain-wall orientations, local rotations, and parent-product interfaces in two-dimensional ferroelastics. Using the approach described here, these results can be extended to two-dimensional improper ferroelastics and three-dimensional proper/improper ferroelastics.

DOI: 10.1103/PhysRevB.68.104105 PACS number(s): 81.30.Kf, 64.70.Kb, 05.70.Fh

I. INTRODUCTION

In many structural transitions one or more components of the strain tensor act as the primary order parameter (POP) driving the transition.[1] To describe various low-symmetry phases and the associated microstructure, a Ginzburg-Landau free energy (GLFE) is expanded in strain components.[2–10] However, this GLFE cannot be directly minimized due to restrictions arising from elastic compatibility which connects all components of the strain tensor through a single differential equation[4–7] in two dimensions (2D) and six equations[3,10] in three dimensions (3D). To accommodate the compatibility constraints, a widely used procedure is to express the GLFE in terms of a single-valued displacement field. The compatibility conditions are then automatically satisfied and the variation with respect to displacements becomes unconstrained.

Our goal has been to obtain a unified description of proper ferroelastic phase transitions based entirely on strain variables.[7,10,11] Here we aim to demonstrate how symmetry can be systematically used to enumerate all possible ferroelastic transitions in 2D and obtain the resulting free energies as well as various aspects of microstructure. The strain-based formalism uses strain as the primary order parameter, provides Landau polynomial free-energy invariants, and the Ginzburg gradient terms. The Landau free energy is anharmonic (F_0) in terms of the POP and harmonic (F_{sec}) in the secondary OP strains.[11,12] When the GLFE is minimized in the context of the compatibility constraint, the secondary OP strain components can be eliminated and the GLFE can be expressed solely in terms of the POP strain components. By substitution, the harmonic term F_{sec} then becomes an anisotropic long-range interaction[6,7,10,11] between these primary strain components, induced by the compatibility relations.

Given this (static) GLFE, which is a function of the strain POP *only*, we should be able to determine the low-symmetry phases and the (static) microstructure. In addition, there are important structural characteristics embodied within these compatibility kernels. In this paper we demonstrate in 2D that through the use of symmetry we can (i) comprehensively enumerate all ferroelastic species, (ii) obtain values of the OP (strains) in different domains, (iii) identify domain pair classes, (iv) determine allowed domain-wall orientations, (v) calculate local rotations for different domain walls, (vi) predict habit plane (parent-product interface) orientations, and finally (vii) describe features of microstructure for 2D ferroelastic transitions. It is important to note that a POP *strain only* GL treatment captures the essential physics since the kernels embody both material aspects (through elastic constants) and crystal symmetry attributes, as well as the long-range elastic interaction. Thus, this formalism contains the necessary information for predicting orientation features of microstructure. In the following, we will use the *ISOTROPY* software by Stokes and Hatch,[13] which is developed for 3D but through projection it applies equally well to the description of structures in 2D.

II. FORMALISM

All crystalline structures in 2D have a symmetry defined by one of 17 two-dimensional space groups. In Table I, we list these structural symmetries and give the corresponding 3D space group which yields the 2D symmetry upon projection along the principal axis. [In the lattice column we give the lattice type (e.g., OP represents oblique primitive, etc.) and in parenthesis the space-group identification number as given according to the International Tables for Crystallography.[14]] A proper ferroelastic transition takes place when the product phase results from the onset of new strain components and this resultant strain can be reoriented from one domain of the product phase to another. We do not consider improper ferroelastic transitions here in which strain acts as a secondary order parameter and some other physical variable (e.g., shuffle, polarization, magnetization) drives the transition.

In Table II we list the proper ferroelastic transitions that are allowed in 2D. Note that there may be more than one product phase and thus more than one ferroelastic transition from a given parent. In column 2 the resulting subgroup is indicated. In column 3 we indicate the irreducible representation (IR) form of the POP (i.e., the relevant strain tensor

TABLE I. Correspondence between two-dimensional and three-dimensional space groups (SG). For the lattice specification, O, oblique; R, rectangular; S, square; H, hexagonal; P, primitive; and C=centered.

2D SG	Lattice	3D SG
$p6mm(17)$	HP	$P6mm(183)$
$p6(16)$	HP	$P6(168)$
$p31m(15)$	HP	$P31m(157)$
$p3m1(14)$	HP	$P3m1(156)$
$p3(13)$	HP	$P3(143)$
$p4gm(12)$	SP	$P4bm(100)$
$p4mm(11)$	SP	$P4mm(99)$
$p4(10)$	SP	$P4(75)$
$c2mm(9)$	RC	$Cmm2(35)$
$p2gg(8)$	RP	$Pba2(32)$
$p2mg(7)$	RP	$Pma2(28)$
$p2mm(6)$	RP	$Pmm2(25)$
$cm(5)$	RC	$Bm(8)$
$pg(4)$	RP	$Pb(7)$
$pm(3)$	RP	$Pm(6)$
$p2(2)$	OP	$P2(3)$
$p1(1)$	OP	$P1(1)$

TABLE II. 23 Proper ferroelastic transitions in 2D.

Parent	Subgroups	Primary IR
$p6mm(17)$	$c2mm(9)$, $p2(2)$	$\Gamma_5=(\epsilon_2,-\epsilon_3)$
$p6(16)$	$p2(2)$	$\Gamma_3\Gamma_5=(\epsilon_2,-\epsilon_3)$
$p31m(15)$	$cm(5)$, $p1(1)$	$\Gamma_3=(\epsilon_2,-\epsilon_3)$
$p3m1(14)$	$cm(5)$, $p1(1)$	$\Gamma_3=(\epsilon_2,-\epsilon_3)$
$p3(13)$	$p1(1)$	$\Gamma_2\Gamma_3=(\epsilon_2,-\epsilon_3)$
$p4gm(12)$	$p2gg(8)$	$\Gamma_2=(\epsilon_2)$
	$c2mm(9)$	$\Gamma_3=(\epsilon_3)$
	$p2(2)$	$\Gamma_2+\Gamma_3=(\epsilon_2;\epsilon_3)$
$p4mm(11)$	$p2mm(6)$	$\Gamma_2=(\epsilon_2)$
	$c2mm(9)$	$\Gamma_3=(\epsilon_3)$
	$p2(2)$	$\Gamma_2+\Gamma_3=(\epsilon_2;\epsilon_3)$
$p4(10)$	$p2(2)$	$\Gamma_2+\Gamma_3=(\epsilon_2;\epsilon_3)$
$c2mm(9)$	$p2(2)$	$\Gamma_2=(\epsilon_3)$
$p2gg(8)$	$p2(2)$	$\Gamma_2=(\epsilon_3)$
$p2mg(7)$	$p2(2)$	$\Gamma_2=(\epsilon_3)$
$p2mm(6)$	$p2(2)$	$\Gamma_2=(\epsilon_3)$
$cm(5)$	$p1(1)$	$\Gamma_2=(\epsilon_3)$
$pg(4)$	$p1(1)$	$\Gamma_2=(\epsilon_3)$
$pm(3)$	$p1(1)$	$\Gamma_2=(\epsilon_3)$
$p2(2)$	$p1(1)$	$\Gamma_2=(\epsilon_3)$

components ϵ_2 and ϵ_3) which induces the ferroelastic transition. The additional strain components are secondary OP's. Throughout this development we use the symmetry adapted forms for strain $\epsilon_1=\frac{1}{2}(u_{x,x}+u_{y,y})$, $\epsilon_2=\frac{1}{2}(u_{x,x}-u_{y,y})$, and $\epsilon_3=\frac{1}{2}(u_{x,y}+u_{y,x})$. [The associated local rotation is $\omega_3=\frac{1}{2}(u_{x,y}-u_{y,x})$.] The corresponding IR's for strain are denoted by Γ_i. In two cases ($\Gamma_3\Gamma_5$ and $\Gamma_2\Gamma_3$) a two-dimensional sum of IR's drives the transition. The physically irreducible representation is composed of two IR's neither one of which can be chosen real.[13] In three cases (of the form $\Gamma_2+\Gamma_3$) two one-dimensional IR's simultaneously drive the transition and the associated (coupled POP) strain components are separated by a semicolon. We emphasize that the three low-symmetry rectangular subgroups $pm(3)$, $pg(4)$, and $p2mg(7)$ cannot be obtained as a product phase in a 2D proper ferroelastic transition. It is through the 2D to 3D correspondence that ISOTROPY[13] was used and the identification of the appropriate IR OP form was made. Note that there are 23 ferroelastic transitions in 2D in contrast to 94 in 3D.[15] Also note that an oblique→oblique transition ($p2\rightarrow p1$) is allowed in 2D. There is no ferroelastic transition within the same crystal system in 3D, e.g., a triclinic→triclinic is not allowed.

The above 23 transitions correspond to 12 ferroelastic species: $6mmF2mm(3)$, $6mmF2(6)$, $6F2(3)$, $3mFm(3)$, $3mF1(6)$, $3F1(3)$, $4mmF2mm(2)$, $4mmF2(4)$, $4F2(2)$, $2mmF2(2)$, $mF1(2)$, and $2F1(2)$. The notation follows that of Aizu.[15] On the left is the point group of the parent and on the right the point group of the product phase. They are separated by the letter F representing ''ferroelastic.'' Each species will determine a number of symmetry related domains (i.e., variants). The number of domains is given above in parenthesis. Pairs of domains can be collected into classes[16] where each member of the class is crystallographically equivalent to any other in the class. From the viewpoint of energy and OP profiles, we need only consider one representative member of each class.[17,18] This representative domain pair will then determine allowed domain wall orientations and energies from which any other pair (and its domain-wall orientations) in the class can be obtained by a parent symmetry element.

III. PROTOTYPE EXAMPLE

We will illustrate our procedure of using strain variables to describe the transition. To have a specific example in mind, we consider the first entry in Table II. This corresponds to the $6mmF2mm(3)$ ferroelastic species mentioned above. This transition takes a triangular lattice to a centered rectangular lattice with three orientational states of the latter. The POP (see column 3 of Table II) is a two-component shear $\Gamma_5=(\epsilon_2,-\epsilon_3)$ and the secondary OP is the dilatation $\Gamma_1=(\epsilon_1)$. The (hexagonal) free energy for this transition, to fourth degree in POP and to second degree in secondary OP's, is given in Table III and the compatibility equation for all transitions in 2D is of the form $G\equiv(\partial_2^2+\partial_1^2)\epsilon_1+(\partial_2^2-\partial_1^2)\epsilon_2-2\partial_1\partial_2\epsilon_3=0$. The free energy consists of three parts; $F=F_L+F_C+F_G$, the Landau term without coupling (F_L), the part with coupling between the POP and secondary OP's (F_C), and the Ginzburg part containing gradients of the POP (F_G). Since a third-order invariant is allowed in F_L, this transition is of first order. It is straightforward to include sixth degree terms in the POP for those first-order transitions in which a third-order invariant is not symmetry allowed.[13] The Landau term is further written as $F_L=F_0+F_{sec}$, where F_0 (F_{sec}) depends upon the POP (secondary OP).

TABLE III. Free-energy invariants for all 2D ferroelastic transitions. For simplicity, summation in coordinate space on the right has been dropped.

Rectangle and oblique:
$F_L = A_1^{(1)} u_{x,x}^2/2 + A_1^{(2)} u_{y,y}^2/2 + A_1^{(3)} \epsilon_2^2/2 + A_2^{(3)} \epsilon_2^4/4$
$F_C = C_1 u_{x,x} \epsilon_2^2 + C_2 u_{y,y} \epsilon_2^2$
$F_G = g_1 \epsilon_{2,x}^2 + g_2 \epsilon_{2,y}^2$
Square:
$F_L = A_1^{(1)} \epsilon_1^2/2 + A_1^{(2)} \epsilon_2^2/2 + A_2^{(2)} \epsilon_2^4/2 + A_1^{(3)} \epsilon_3^2/2 + A_2^{(3)} \epsilon_3^4/2$
$F_C = C_1 \epsilon_1 \epsilon_2^2 + C_2 \epsilon_1 \epsilon_3^2 + C_3 \epsilon_2^2 \epsilon_3^2$
$F_G = g_1(\epsilon_{2,x}^2 + \epsilon_{2,y}^2) + g_2(\epsilon_{3,x}^2 + \epsilon_{3,y}^2) + g_3(\epsilon_{2,x}\epsilon_{3,y} + \epsilon_{2,y}\epsilon_{3,x})$
Hexagonal:
$F_L = A_1^{(1)} \epsilon_1^2/2 + A_1^{(2)}(\epsilon_2^2 + \epsilon_3^2)/2 + A_2^{(2)}(\epsilon_3^3 - 3\epsilon_2^2\epsilon_3)/3$
$+ A_3^{(2)}(\epsilon_2^2 + \epsilon_3^2)^2/4$
$F_C = C_1 \epsilon_1(\epsilon_2^2 + \epsilon_3^2)$
$F_G = g_1(3\epsilon_{2,x}^2 + 2\epsilon_{2,x}\epsilon_{3,y} + \epsilon_{2,y}^2 + 2\epsilon_{2,y}\epsilon_{3,x} + \epsilon_{3,x}^2 + 3\epsilon_{3,y}^2)$
$+ g_2(\epsilon_{2,x}^2 + 6\epsilon_{2,x}\epsilon_{3,y} - \epsilon_{2,y}^2 - 2\epsilon_{2,y}\epsilon_{3,x} - \epsilon_{3,x}^2 + \epsilon_{3,y}^2)$
$+ g_3(\epsilon_{2,x}^2 - 2\epsilon_{2,x}\epsilon_{3,y} + 3\epsilon_{2,y}^2 - 2\epsilon_{2,y}\epsilon_{3,x} + 3\epsilon_{3,x}^2 + \epsilon_{3,y}^2)$

The Euler-Lagrange variation of $[F - \Sigma \Lambda G]$ with respect to the secondary OP's is then[7] $\delta(F_{sec} - \Sigma \Lambda G)/\delta \epsilon_1 = 0$. (The notion of such variation for the square to rectangle transition was presented in Ref. 6.) In a spatially inhomogeneous structure the order parameters become dependent on position. The free energy then changes to a spatial sum over these local contributions to the free-energy density, which becomes a sum over wave vectors in Fourier space. In this hexagonal case, for example, $F_{sec} \equiv \Sigma_r f_{sec}(\vec{r}) = \Sigma_r A_1^{(1)} \epsilon_1^2/2$. Here $A_1^{(1)}$ is the bulk modulus, one of the relevant elastic constants $A_i^{(j)}$ of Table III. The variation gives (in k space assuming periodic boundary conditions) $\epsilon_1(\vec{k}) = (k_x^2 + k_y^2)\Lambda(\vec{k})/A_1^{(1)}$. We then substitute $\epsilon_1(\vec{k})$ back into the compatibility constraint condition and solve for the Lagrange multiplier $\Lambda(\vec{k})$. Thus, $e_1(\vec{k})$ is expressed in terms of $\epsilon_2(\vec{k})$, $\epsilon_3(\vec{k})$ and in Fourier space

$$f_{sec}(\vec{k}) \equiv (1/2) A_1^{(1)} \sum_{\ell,\ell'} U_{\ell\ell'}(\vec{k}) \epsilon_\ell(\vec{k}) \epsilon_{\ell'}^*(\vec{k}),$$

where $f_{sec}(\vec{k}) = A_1^{(1)} |(k_x^2 - k_y^2)\epsilon_2/k^2 + 2k_x^2 k_y^2 \epsilon_3/k^2|^2/2$. The (static) "compatibility kernel" $U(\vec{k})$ is independent of $|\vec{k}|$ at long wavelengths: $U(\vec{k}) \to U(\hat{k})$. Hence, in coordinate space this is an anisotropic long-range ($\sim 1/r^D$, with $D=2$) potential mediating the elastic interactions of the POP.

There are three possible domains in the product phase (i.e., three centered rectangular orientations) corresponding to POP directions $(a,0), (-(1/2)a, -(\sqrt{3}/2)a)$, and $(-(1/2)a, (\sqrt{3}/2)a)$, with a denoting an arbitrary constant.[9] Among these three orientations, there is only one class of domain pairs and for simplicity we take the pair consisting of the second and third orientation states (2,3) as representative of the class.

The boundary conditions for this pair are at $-\infty$; $a = -a_0/2$, $b = -\sqrt{3}a_0/2$, $\epsilon_1 = 0$, $\omega_3 = -\Omega$ and at $+\infty$; $a = -a_0/2$, $b = \sqrt{3}a_0/2$, $\epsilon_1 = 0$, $\omega_3 = +\Omega$. Elastic compatibility implies that $\Omega = \sqrt{3}a_0/2$. Thus, there are opposite rotations in the two domains. The POP strain profile through the domain-wall interface can be obtained by solving the appropriate differential equations under these boundary conditions. At some specific temperature (i.e., a specific value of the coefficient of the harmonic POP term at which the domain-wall problem becomes one dimensional) in each case an analytic form for the domain wall can be obtained.[18]

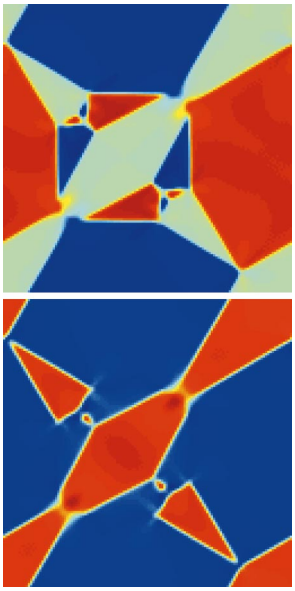

FIG. 1. (Color) Example of microstructure for the $6mmF2mm(3)$ ferroelastic transition for which the POP (see column 3 of Table II) is a two-component shear $\Gamma_5 = (\epsilon_2, -\epsilon_3)$. Top: The three values of the shear strain ϵ_3 are color coded with red (positive), blue (negative), and green (zero). Note the domain-wall orientations with angles that are multiples of $\pi/6$ and $\pi/3$. Bottom: The two values of the deviatoric shear ϵ_2 are shown with red (positive) and blue (negative).

Figure 1 shows typical (static) microstructure for this $6mmF2mm(3)$ transition. The shear strains ϵ_3 are displayed in Fig. 1 (Top) with the color coding representing positive (red), negative (blue), and zero (green) strain values associated with the three centered rectangular orientations. The two positive (red) and negative (blue) values of ϵ_2 are shown in Fig. 1 (bottom). The domain-wall orientations correspond to multiples of $\pi/6$ and $\pi/3$. The structures were obtained by relaxing the free energy using a time-dependent Ginzburg Landau (TDGL) equation.[7,11] The emphasis here is not on dynamics, but on examples of typical "equilibrium" structures and the TDGL is one way of obtaining these textured configurations.[11] Such microstructure has been seen using phase contrast microscopy on lead orthovanadate[19] and has been simulated by other methods.[8,20]

Note that if we consider the first entry in Table II but a different ferroelastic species $6mmF2$, we will get six oblique ($p2$) orientational states in the product phase. However, the free energy will be the same, to this order of expansion, as given in Table III. All 23 ferroelastic transitions in 2D can be described by three GLFE forms (if we limit the degree of expansion in strain and neglect additional second-

TABLE IV. Representative elastic compatibility kernels $U_{\ell\ell'}(\vec{k})$ for all 2D ferroelastic transitions for interaction between POP through the free energy $F_{sec}=(1/2)\Sigma_{\ell\ell',k}U_{\ell\ell'}\epsilon_\ell\epsilon^*_{\ell'}\equiv\Sigma_k f_{sec}(\vec{k})$. Here $\epsilon_2=\frac{1}{2}(u_{x,x}-u_{y,y})$ and $\epsilon_3=\frac{1}{2}(u_{x,y}+u_{y,x})$.

Rectangular and oblique to oblique:
$f_{sec}(\vec{k})=2A_1^{(2)}[k_x^2k_y^2\lvert\epsilon_2\rvert^2]/(k_y^4+A_1^{(2)}k_x^4/A_1^{(1)})$
Square to oblique:
$f_{sec}(\vec{k})=[A_1^{(1)}/2]\lvert(k_x^2-k_y^2)\epsilon_2/k^2+2k_xk_y\epsilon_3/k^2\rvert^2$
Square to rectangle I (deviatoric):
$f_{sec}(\vec{k})=[A_1^{(1)}/2][(k_x^2-k_y^2)^2\lvert\epsilon_2\rvert^2]/[(k_x^2+k_y^2)^2+4A_1^{(1)}k_x^2k_y^2/A_1^{(3)}]$
Square to rectangle II (shear):
$f_{sec}(\vec{k})=[A_1^{(1)}/2][k_x^2k_y^2\lvert\epsilon_3\rvert^2]/[k^4+A_1^{(1)}(k_x^2-k_y^2)^2/A_1^{(2)}]$
Hexagonal to rectangle or oblique:
$f_{sec}(\vec{k})=[A_1^{(1)}/2]\lvert(k_x^2-k_y^2)\epsilon_2/k^2+2k_xk_y\epsilon_3/k^2\rvert^2$

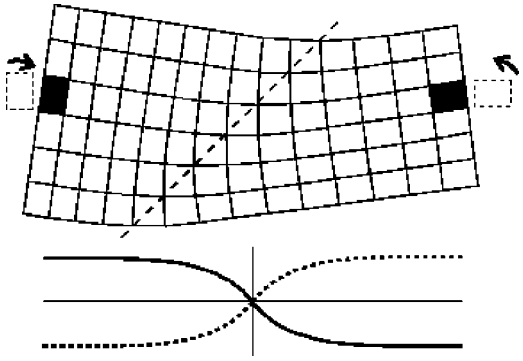

FIG. 2. Example of local rotation (ω_3) of domains for the square to rectangle (I) transition driven by the deviatoric strain. The solitonlike profiles in the lower part of the figure are deviatoric strain (ϵ_2, solid line) interpolating between $\pm\epsilon_0$ and local rotation (dashed line) interpolating between $\mp\Omega_0$, respectively.

ary OP's such as shuffle for crystals without a monatomic basis) and five elastic kernels. The five forms for the kernels are given in Table IV. Note also that rectangular ($p2mm$) $\rightarrow$oblique ($p2$) and oblique ($p2$)$\rightarrow$oblique ($p1$) transitions are described by the same kernel but the strains are defined with respect to a rectangular lattice in the former case and with respect to an oblique lattice in the latter case. In addition, the square$\rightarrow$rectangle transition can be driven either by a deviatoric strain or by a shear strain. The latter leads to a centered rectangular lattice.

In Fig. 2 we illustrate the local (lattice) rotation associated with domain matching for the square to rectangular transition resulting from the deviatoric strain.[4,5] This local rotation is given by $\omega_3=\frac{1}{2}(u_{x,y}-u_{y,x})$, as mentioned earlier. The rotation does not contribute to the free energy. However, it does restrict compatibility of neighboring domains. The slanted

TABLE V. Characteristics of all proper ferroelastic transitions in 2D. $p=\{b+(b^2+a^2)^{1/2}\}/a$, $r=\{3b+\sqrt{3}a+2[3(a^2+b^2)]^{1/2}\}/\{3a-\sqrt{3}b\}$, $s=\{3b-\sqrt{3}a+2[3(a^2+b^2)]^{1/2}\}/\{\sqrt{3}b+3a\}$, $\alpha=\{-b+(b^2+a^2)^{1/2}\}/a$.

Ferroelastic species	Domain values	Pair classes	Wall orientations	Habit plane orientations
$6mmF2mm$	$(a,0)$, $(-a/2,-\sqrt{3}a/2)$, $(-a/2,\sqrt{3}a/2)$	(1,2)	$x=-\sqrt{3}y, x=y/\sqrt{3}$	$x=y, x=-y$
$6mmF2$	(a,b), $(-a/2+\sqrt{3}b/2,-\sqrt{3}a/2-b/2)$	(1,2), (1,3)	$x=sy, x=-y/s; x=ry, x=-y/r;$	$x=\alpha y, x=-y/\alpha$
	$(-a/2-\sqrt{3}b/2,\sqrt{3}a/2-b/2)$	(1,4)	$x=\sqrt{3}y, x=-y/\sqrt{3};$	
	$(-a/2+\sqrt{3}b/2,\sqrt{3}a/2+b/2)$, $(a,-b)$	(1,5)	$x=0, y=0;$	
	$(-a/2-\sqrt{3}b/2,-\sqrt{3}a/2+b/2)$	(1,6)	$x=y/\sqrt{3}, x=-\sqrt{3}y$	
$6F2$	(a,b), $(-a/2,\sqrt{3}a/2)$	(1,2)	$x=ry, x=-y/r;$	$x=\alpha y, x=-y/\alpha$
	$(-a/2+\sqrt{3}b/2,-\sqrt{3}a/2-b/2)$	(1,3)	$x=sy, x=-y/s$	
$3mFm(s)$	$(a,0)$, $(-a/2,\sqrt{3}a/2)$,$(-a/2,-\sqrt{3}a/2)$	(1,2)	$x=\sqrt{3}y, x=-y/\sqrt{3}$	$x=y, x=-y$
$3mF1$	(a,b), $(-a/2-\sqrt{3}b/2,\sqrt{3}a/2-b/2)$,	(1,6), (1,5)	$x=y/\sqrt{3}, x=-y\sqrt{3}; x=\sqrt{3}y,$	$x=y, x=-y$
	$(-a/2+\sqrt{3}b/2,-\sqrt{3}a/2-b/2)$, $(a,-b)$	(1,4), (1,3)	$x=-y/\sqrt{3}; x=0, y=0; x=sy,$	
	$(-a/2+\sqrt{3}b/2,\sqrt{3}a/2+b/2)$,	(1,2)	$x=-y/s; x=ry, x=-y/r$	
	$(-a/2-\sqrt{3}b/2,-\sqrt{3}a/2+b/2)$			
$3F1$	(a,b), $(-a/2-\sqrt{3}b/2,\sqrt{3}a/2-b/2)$	(1,2)	$x=ry, x=-y/r;$	$x=\alpha y, x=-y/\alpha$
	$(-a/2+\sqrt{3}b/2,-\sqrt{3}a/2-b/2)$	(1,3)	$x=sy, x=-y/s$	
$4mmF2mm(p)$	(a), $(-a)$	(1,2)	$x=y, x=-y$	$x=y, x=-y$
$4mmF2mm(s)$	(a), $(-a)$	(1,2)	$x-0, y=0$	$x=0, y=0$
$4mmF2$	(a,b), $(-a,-b)$	(1,2), (1,3)	$x=py, x=-y/p; x=0, y=0;$	$x=\alpha y, x=-y/\alpha$
	$(a,-b)$, $(-a,b)$	(1,4)	$x=y, x=-y$	
$4F2$	(a,b), $(-a,-b)$	(1,2)	$x=py, x=-y/p$	$x=\alpha y, x=-y/\alpha$
	$(a,-b)$, $(-a,b)$			
$2mmF2$	(a), $(-a)$	(1,2)	$x=0, y=0$	$x=0, y=0$
$mF1$	(a), $(-a)$	(1,2)	$x=0, y=0$	$x=0, y=0$
$2F1$	(a), $(-a)$	(1,2)	$x=0, y=0$	$x=0, y=0$

dashed line represents a twin boundary between the two rectangular variants.

In Table V we list the relevant characteristics of all proper ferroelastic transitions in 2D. For each species we have listed the following: (a) in column 2, the OP values for each domain, (b) in column 3, a representative for each of the pair classes (where more than one pair is listed, there is more than one equivalence class of pairs), (c) in column 4, the domain-wall orientations, and (d) in column 5, the habit plane orientations (consistent with those obtained by Boulesteix *et al.*[21]). Other wall orientations are allowed but they are equivalent and easily obtained by the rotations or translations which were lost from the parent structure at the transition. The notation p,s in column 1 refers to the orientation of the ferroelastic crystal relative to the principal axis of the parent structure. The letters ''p'' and ''s'' stand for ''principal'' and ''side,'' respectively. The symmetry considerations given in Table V were obtained using ISOTROPY.[13] These include space-group changes at the transition, order-parameter forms, domain configurations, equivalent and inequivalent pairs, etc.

IV. CONCLUSION

For structural transitions in which strain is the primary order parameter, we have obtained 23 proper ferroelastic transitions in 2D and derived distinct, static elastic compatibility kernel forms. The appropriate Ginzburg-Landau free energies containing both primary and secondary OP's are easily obtained using ISOTROPY.[13] The five anisotropic compatibility kernels have been obtained by an Euler-Lagrange minimization. These kernels embody the essential physics of the microstructure in ferroelastics. In addition to specifying anisotropic, long-range interactions, the kernels influence possible domain-wall orientations, local rotations, and parent-product interfaces in 2D ferroelastics. In a later work, compatibility kernels have been used in an underdamped dynamics.[11]

Our philosophy can also apply to improper ferroelastics (e.g., ferroelectrics or magnetoelastics) when a physical quantity other than strain (such as shuffle, polarization or magnetization) is the POP and strain serves as a secondary OP. In these cases, elastic compatibility leads to an anisotropic long-range interaction (generally) in the higher powers of the nonstrain POP. Our approach can be readily applied to find the orientations of domain walls in the primary OP, e.g., ferroelectric and magnetoelastic walls. Similarly, by exploiting symmetry to the full extent we can obtain similar results in 3D, i.e., prediction of domain-wall orientations for the 94 ferroelastic transitions as well as habit planes.

ACKNOWLEDGMENTS

We are grateful to Yu. B. Gaididei for stimulating discussions. This work was supported by the U.S. Department of Energy.

[1] J.C. Tolédano and P. Tolédano, *The Landau Theory of Phase Transitions* (World Scientific, Singapore, 1987).
[2] R. Kragler, Physica B **93**, 314 (1978).
[3] G.R. Barsch and J.A. Krumhansl, Phys. Rev. Lett. **53**, 1069 (1984).
[4] A.E. Jacobs, Phys. Rev. B **31**, 5984 (1985).
[5] G.R. Barsch and J.A. Krumhansl, Metall. Trans. A **19**, 761 (1988).
[6] S. Kartha, J.A. Krumhansl, J.P. Sethna, and L.K. Wickham, Phys. Rev. B **52**, 803 (1995).
[7] S.R. Shenoy, T. Lookman, A. Saxena, and A.R. Bishop, Phys. Rev. B **60**, R12 537 (1999).
[8] S.H. Curnoe and A.E. Jacobs, Phys. Rev. B **62**, R11 925 (2000); **64**, 064101 (2001).
[9] S.H. Curnoe and A.E. Jacobs, Phys. Rev. B **63**, 094110 (2001).
[10] K.Ø. Rasmussen, T. Lookman, A. Saxena, A.R. Bishop, R.C. Albers, and S.R. Shenoy, Phys. Rev. Lett. **87**, 055704 (2001).
[11] T. Lookman, S.R. Shenoy, K.Ø. Rasmussen, A. Saxena, and A.R. Bishop, Phys. Rev. B **67**, 024114 (2003).
[12] There is another (slightly different) usage for the secondary OP for proper ferroelastics in the literature. The secondary OP strains have been called non-OP strains, e.g., in Refs. 7 and 10.
[13] H.T. Stokes and D.M. Hatch, *Isotropy Subgroups of the 230 Crystallographic Space Groups* (World Scientific, Singapore, 1988). The software package ISOTROPY is available at http://www.physics.byu.edu/~stokesh/isotropy.html, ISOTROPY (1991).
[14] *International Tables for Crystallography*, edited by T. Hahn (Reidel, Boston, 1983).
[15] K. Aizu, J. Phys. Soc. Jpn. **27**, 387 (1969).
[16] R.A. Hatt and D.M. Hatch, Ferroelectrics **226**, 61 (1998).
[17] D.M. Hatch, P. Hu, A. Saxena, and G.R. Barsch, Phys. Rev. Lett. **76**, 1288 (1996).
[18] See, e.g. (even for a six-component order parameter) W. Cao, A. Saxena, and D.M. Hatch, Phys. Rev. B **64**, 024106 (2001); D.M. Hatch, W. Cao, and A. Saxena, *ibid.* **65**, 094110 (2002).
[19] C. Manolikas and S. Amelinckx, Phys. Status Solidi A **60**, 607 (1980).
[20] Y.H. Wen, Y.Z. Wang, and L.Q. Chen, Philos. Mag. A **80**, 1967 (2000).
[21] C. Boulesteix, B. Yangui, M. Ben Salem, C. Manolikas, and S. Amelinckx, J. Phys. **47**, 461 (1986).